TECHNOLOGIE 5G

Bulletin de veille scientifique : Février 2025

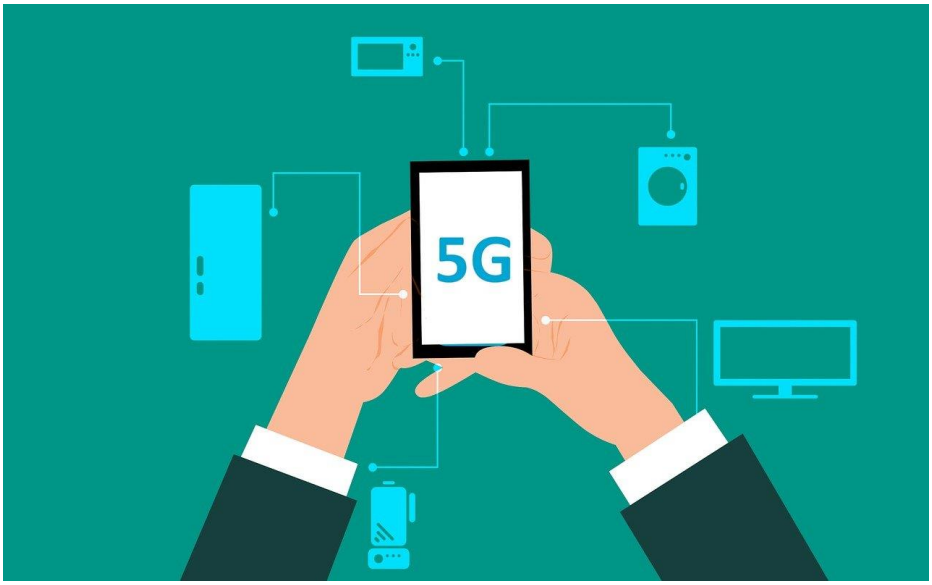

Objectifs : réaliser une veille scientifique sur la technologie 5G

La validation des informations fournies (exactitude, fiabilité, pertinence par rapport aux principes de prévention, etc.) est du ressort des auteurs des articles signalés dans la veille. Les informations ne sont pas le reflet de la position de l'INRS. Les éléments issus de cette veille sont founis sans garantie d'exhaustivité. Les liens mentionnés dans le bulletin donnent accès aux documents sous réserve d'un abonnement à la ressource.

Les bulletins de veille sont disponibles sur le portail documentaire de l'INRS. L'abonnement permet de recevoir une alerte mail lors de la publication d'un nouveau bulletin (bouton « M'abonner » disponible après connexion à son compte).

Généralités

Aucun article dans ce bulletin.

Performances et sécurité

Compressive transmission scheme for power regulation of embedded 5G communication devices.

Zhu M, Liu X, Ye Z, Othmen S, Alfahid A, Flah A, et al. *Sci Rep*. 2025 Feb 18;15(1):5889.

Power management for embedded devices in Fifth Generation (5G) networks is mandatory for synchronizing the communication between the devices. In such cases, the need for integration power optimization is recommended aiding lossless and high-speed communications. To suppress the issues in embedded hardware-based power failures during transmissions, this article proposes a Compressive Transmission Scheme (CTS) through Power Regulation (PR). The proposed scheme identifies multiple transmission possibilities under low power and high throughput constraints of 5G in a single interval. The device integrations are decided by the available devices under power-efficient transmission slots. Such allocation slots are defined for integrated transmission using neural-diffracted networks. The learning network defines the objectives for transmission between embedded hardware and the 5G device under low power. This is pursued until the transmission is completed; the adverse energy drain impact is handled by offloading the slots to the active hardware available. This balances the power management to prevent communication loss satisfying the 5G constraints. For the maximum slots/device, the proposed scheme achieves 11.46% high slot allocation, 12.47% low latency, and 9.99% less power consumption.

Lien vers l'article

Statistical-based detection of pilot contamination attack for NOMA in 5G networks.

Nashat D, Khairy S. *Sci Rep*. 2025 Jan 29;15(1):3726.

Fifth-generation (5G) communication technologies, such as millimeter wave communication, massive multiple-input-multiple-output and non-orthogonal-multiple-access (NOMA) are playing a pivotal role in promoting the modern applications of the Internet-of-Things. Using non-orthogonal resource allocation, NOMA can increase spectrum efficiency and achieve wide connectivity with low transmission delay and signaling cost. Despite the high potential of NOMA in 5G communications, NOMA is susceptible to a pilot contamination attack (PCA), in which an attacker resents the same pilot signals as authorized users. Currently, using the available detection methods in NOMA gives high false positive probability since the time-division-duplex or orthogonal resource block can be allocated by many authorized user. Since the pilot contamination attack changes the signal reception at the legitimate receiver, this work introduces a novel detection scheme for identifying Pilot Contamination attack (PCA) that statistically investigates the asymmetry in received signal power levels. The main idea of the proposed detection scheme is to use various statistical measurements for normal traffic attributes (CSI) as a reference profile. Then, compute the Mahalanobis distance between the reference profile and CSI for the incoming connection and use the probability of the uniform distribution to make the final detection decision. The performance of the proposed detection technique in terms of its detection rate and false positive probabilities has been evaluated through extensive simulation. The simulation results show that the proposed scheme succeeded in detecting the pilot contamination attack with a detection rate of up to 98% and a precision reached 97.88%.

Lien vers l'article

Multi-Source, Fault-Tolerant, and Robust Navigation Method for Tightly Coupled GNSS/5G/IMU System.

Deng Z, Zhang Z, Ding Z, Liu B. *Sensors (Basel)*. 2025 Feb 5;25(3).

The global navigation satellite system (GNSS) struggles to deliver the precision and reliability required for positioning, navigation, and timing (PNT) services in environments with severe interference. Fifth-generation (5G) cellular networks, with their low latency, high bandwidth, and large capacity, offer a robust communication infrastructure, enabling 5G base stations (BSs) to extend coverage into regions where traditional GNSSs face significant challenges. However, frequent multi-sensor faults, including missing alarm thresholds, uncontrolled error accumulation, and delayed warnings, hinder the adaptability of navigation systems to the dynamic multi-source information of complex scenarios. This study introduces an advanced, tightly coupled GNSS/5G/IMU integration framework designed for distributed PNT systems, providing all-source fault detection with weighted, robust adaptive filtering. A weighted, robust adaptive filter (MCC-WRAF), grounded in the maximum correntropy criterion, was developed to suppress fault propagation, relax Gaussian noise constraints, and improve the efficiency of observational weight distribution in multi-source fusion scenarios. Moreover, we derived the intrinsic relationships of filtering innovations within wireless measurement models and proposed a time-sequential, observation-driven full-source FDE and sensor recovery validation strategy. This approach employs a sliding window which expands innovation vectors temporally based on source encoding, enabling real-time validation of isolated faulty sensors and adaptive adjustment of observational data in integrated navigation solutions. Additionally, a covariance-optimal, inflation-based integrity protection mechanism was introduced, offering rigorous evaluations of distributed PNT service availability. The experimental validation was carried out in a typical outdoor scenario, and the results highlight the proposed method's ability to mitigate undetected fault impacts, improve detection sensitivity, and significantly reduce alarm response times across step, ramp, and multi-fault mixed scenarios. Additionally, the dynamic positioning accuracy of the fusion navigation system improved to 0.83 m (1σ). Compared with standard Kalman filtering (EKF) and advanced multi-rate Kalman filtering (MRAKF), the proposed algorithm achieved 28.3% and 53.1% improvements in its 1σ error, respectively, significantly enhancing the accuracy and reliability of the multi-source fusion navigation system.

Lien vers l'article

Antennes

An All-Metal Broadband Low SLL slot array antenna for use in 5G Sub-6 GHz networks.

Zarifi D, Farahbakhsh A, Mrozowski M. *Sci Rep*. 2025 Feb 19;15(1):6004.

This paper describes the design and implementation of an all-metal wideband cavity-backed slot array antenna specifically optimized for 5G sub-6 GHz networks. The antenna is engineered to feature low sidelobe levels (SLL), which enhance signal clarity and reduce interference. The proposed antenna utilizes a novel approach, directly exciting all radiating slots through the cavity layer, thus eliminating the need for a complex and lossy power dividing network. The antenna's performance is validated through full-wave simulations and measurements. The results demonstrate antenna's ability to achieve wideband operation from 3.1 to 4 GHz with - 19 dB SLL, peak gain of 20.2 dBi, and more than 90% total efficiency. The main advantages provided by the proposed slot arrays are wide bandwidth,

high radiation efficiency, high gain, low sidelobe levels. The all-metal construction ensures robust power handling, and the simplified design contributes to its low complexity. These characteristics make the antenna a promising candidate for 5G deployments.

Lien vers l'article

A pocket-integrated miniature, dual-band, and high gain textile MIMO antenna for 5G and WiFi wearable applications.

Sharma D, Tiwari RN, Singh DK, Matekovits L. *Sci Rep*. 2025 Feb 11;15(1):5061.

This paper reports a miniature low-profile denim textile 2-port MIMO (multiple-input-multiple-output) antenna for dual-bands: 5G sub-6 3.5 GHz and Wi-Fi 5.2 GHz wearable applications. This MIMO antenna has impedance bandwidths and peak gain of 310 MHz and 8.3 dBi and 950 MHz 13.0 dBi at 3.5 and 5.2 GHz, respectively. This MIMO antenna has a compact area of 0.078 λ(0)(2), with both antenna elements of the MIMO being a modified elliptical patch, L-shaped stubs for impedance matching, and a circular decoupling ring to achieve > 25 dB port isolation. The designed antenna is very tiny and integrated into the shirt's pocket. It is tested in two positions, i.e., hidden (integrated inside the pocket, for example, military applications) and visible (when integrated on the pocket surface for conventional communication). Moreover, the antenna's working is analyzed in these positions (hidden and visible), and it was found that it functions well in both 5G sub-6 GHz and Wi-Fi frequency bands with nearly close gain values and communication range. This MIMO antenna has a very small ECC (envelope correlation coefficient) of 0.006/0.002 in both frequency bands, which shows high channel isolation. The 1 gm/10 gm SAR (specific absorption rate) values at 3.5 and 5.2 GHz are 0.034/0.057 and 0.026/0.0132 W/Kg, respectively, substantially lesser than the recommended values of FCC/ICNIRP.

Lien vers l'article

Architecture réseau

Aucun article dans ce bulletin.

Efficacité énergétique

Aucun article dans ce bulletin.

Design and fabrication of an ultra small quadband diplexer integrated with a diplexed power amplifier for mid band 5G applications.

Khani S, Roshani S, Roshani S, Fouladian M. *Sci Rep*. 2025 Feb 11;15(1):5087.

This paper presents a theoretical design strategy for an ultra-small diplexer optimized for fifth-generation (5G) communication systems. The diplexer design includes a dual-band band-pass filter comprising coupled lines, transmission lines (TLs), and two proposed resonators. These resonator configurations are analyzed for enhanced optimization and structural clarity. Even and odd mode analysis, along with the examination of the LC equivalent circuit, is used to determine the TL parameters. The proposed diplexer operates effectively across four 5G mid-range frequency bands, enabled by the proposed band-pass filter. It functions at 1.08, 1.17, 2, and 2.18 GHz, achieving S(21) values of -1.18, -1.24, -1.24, and - 1.37 dB, respectively, at these frequencies. The final power amplifier circuit benefits from the described diplexer due to its compact size (8.1 mm × 19.4 mm). The proposed power amplifier demonstrates operation at these frequencies of 1.08, 1.17, 2, and 2.18 GHz with a power-added efficiency (PAE) of approximately 63% and a drain efficiency (DE) of about 64%. These results show the proper performance of the proposed diplexer and power amplifier for mid-band 5G applications.

Lien vers l'article

Applications médicales et industrielles de la 5G

Applications industrielles

Aucun article dans ce bulletin.

Applications médicales

The impact of a 5G-based smart nursing information system and associated mobile hardware on clinical nurses' work stress: a randomized controlled study in a Chinese hospital.

Ruan X, Lou Y, Zhang X, Wu Z, Yuan H. *Biomed Eng Online*. 2025 Feb 8;24(1):15.

BACKGROUND: Clinical nurses frequently endure substantial work-related stress, adversely affecting their well-being and potentially compromising patient care quality and safety. The integration of a 5G-based medical private network into smart nursing systems and mobile devices offers a promising solution to reduce this stress. This study evaluates the impact of a Smart Nursing Information System based on a 5G Medical Private Network and its Supporting Mobile Hardware (SNIS-SMH) on mitigating work-related stress among clinical nurses. The goal is to provide a scientific basis for nursing management, reduce error incidents, advance nursing procedures, and enhance productivity. RESULTS: A total of 226 nurses completed the study. The SNIS-SMH group showed significantly lower total work stress scores (66.16 ± 9.82) compared to the control group (70.65 ± 11.32, P = 0.002). In specific dimensions, the SNIS-SMH group had lower scores for nursing profession and work (14.17 ± 2.37 vs. 15.00 ± 3.06, P = 0.023), workload and time distribution (10.56 ± 2.45 vs. 12.42 ± 2.55, P < 0.001), and patient care (22.55 ± 3.34 vs. 23.70 ± 4.06, P = 0.021). No significant differences were found in the work environment and resource, and management and interpersonal relationships dimensions. CONCLUSIONS: The SNIS-SMH system significantly alleviated work-related stress among clinical nurses, particularly in nursing duties, workload and time distribution, and patient care.

Lien vers l'article

Application of and research on 5G mobile nursing stations in clinical settings.

Li C, Li L, Li J, Huang R, Qin J, Chen L, et al. *BMC Nurs*. 2025 Feb 7;24(1):146.

OBJECTIVE: This study investigated the application of and research on 5G mobile nursing stations in clinical settings. METHODS: A randomized sample of 300 nurses from one hospital was selected. The control group was established from December 2021 to September 2022 as the nurses used the computerized hospital information system (HIS) for nursing documentation and performed routine manual verification of the treatment and patient information. The observation group was established from October 2022 to August 2023 as the nurses used portable digital assistants (PDAs) from the 5G mobile nursing stations for nursing documentation and scanned quick response (QR) codes to verify treatment and patient information. This study compared the time taken by nurses in both scenarios to verify oral medicine dispensing and intravenous (IV) infusions against medical orders, as well as the time taken by nurses to input vital signs and complete nursing documentation. RESULTS: In the observation group, the average time for verifying IV infusions against medical orders was

52.34 ± 2.61 s, that for verifying oral medicine dispensing against medical orders was 29.32 ± 1.71 s, that for inputting vital signs was 46.82 ± 3.64 s, and that for completing nursing documentation was 86.81 ± 5.62 s. These times were significantly different from those of the control group, which were 59.84 ± 5.76 s, 35.30 ± 2.31 s, 58.58 ± 3.59 s, and 128.51 ± 6.19 s, respectively ($P < 0.05$). CONCLUSIONS: The use of 5G mobile nursing station PDAs to scan QR codes to verify oral medicine dispensing, IV infusions, other treatments, and patient information resulted in faster verification speeds and 100% accuracy, ensuring accurate treatment information verification and patient safety. Moreover, the use of 5G mobile nursing station PDAs for nursing documentation shortened the time for nurses to input vital signs and complete nursing documentation, thereby improving their efficiency in completing documentation tasks and allowing them to devote more time to patients.

Lien vers l'article

Evaluation (Mesure des niveaux d'exposition)

Méthodes d'évaluation

Aucun article dans ce bulletin.

Evaluation population générale

Aucun article dans ce bulletin.

Risques professionnels

Aucun article dans ce bulletin.

Effets biologiques et sur la santé

In silico

Aucun article dans ce bulletin.

In vitro

Aucun article dans ce bulletin.

Sur l'animal

Impact of Microwave Exposure on Cynomolgus Monkeys: EEG and ECG Analysis.

Ma L, Qiao N, Zou Y, Wang H, Wang Y, Zhi W, et al. *Bioelectromagnetics*. 2025 Feb;46(2):e70000.

The annual increase of microwave exposure in human environments continues to fuel debates regarding its potential health impacts. This study monitored the EEG and ECG responses of three Cynomolgus monkeys before and at 0, 3, 7, 14, and 30 days after exposure to 50 mW/cm² microwave radiation for 15 min. The findings revealed no significant differences in the power spectral densities (PSDs) of the whole brain, frontal, and temporal lobes across various frequency bands (δ, θ, α, β, low-γ, and high-γ) immediately and up to 30 days postexposure. Notable alterations were observed primarily at 14 days in the PSDs of the parietal lobe, prefrontal cortex, central zone, and occipital lobe, particularly in the θ and α bands. By Day 30, these values returned to normal ranges. ECG alterations were characterized by changes in T-wave shape and amplitude. One monkey exhibited bidirectional spikes at 7 and 14 days that normalized by Day 30. Another showed similar patterns with reduced amplitude, and a third monkey displayed a towering forward wave at 14 days that persisted at 30 days. In conclusion, the administration of L-band microwave radiation at the specified dose did not result in immediate alterations to EEG and ECG, but it induced transient modifications in brain electrical activity and normalized after 30 days, which contributed to evaluate the health implications of microwave exposure in humans.

Lien vers l'article

Numerical dosimetry of specific absorption rate of insects exposed to far-field radiofrequency electromagnetic fields.

Jeladze V, Nozadze T, Partsvania B, Thielens A, Shoshiashvili L, Gogoladze T. *Int J Radiat Biol*. 2025;101(3):327-40.

PURPOSE: This paper reports a study of electromagnetic field (EMF) exposure of several adult insects: a ladybug, a honey bee worker, a wasp, and a mantis at frequencies ranging from 2.5 to 100 GHz. The purpose was to estimate the specific absorption rate (SAR) in insect tissues, including the brain, in

order to predict the possible biological effects caused by EMF energy absorption. METHOD: Numerical dosimetry was executed using the finite-difference time-domain (FDTD) method. Insects were modeled as 3-tissue heterogeneous dielectric objects, including the cuticle, the inner tissue, and the brain tissue. The EMF source was modeled as sinusoidal plane waves at a single frequency (far-field exposure). RESULTS: The whole-body averaged, tissue averaged, and 1 milligram SAR values were determined in insects for all considered frequencies for 10 different incident plane waves. SAR values were normalized to the incident power density of 1 mW/cm(2). Maximal EMF absorption in the inner and brain tissues was observed at 6, 12, and 25 GHz for the considered insects, except the brain tissue of a ladybug (max at 60 GHz). CONCLUSION: The paper presented the first estimation of the SAR for multiple insects over a wide range of RF frequencies using 3-tissue heterogenous insect 3D models created for this specific research. The selection of tissues' dielectric properties was validated. The obtained results showed that EMF energy absorption in insects highly depends on frequency, polarization, and insect morphology.

Lien vers l'article

Sur l'homme

The effect of exposure to radiofrequency fields on cancer risk in the general and working population: A systematic review of human observational studies - Part II: Less researched outcomes.

Karipidis K, Baaken D, Loney T, Blettner M, Mate R, Brzozek C, et al. *Environ Int*. 2025 Feb;196:109274.

BACKGROUND: In the framework of the World Health Organization assessment of health effects of exposure to radiofrequency electromagnetic fields (RF-EMF), we have conducted a systematic review of human observational studies on the association between exposure to RF-EMF and risk of neoplastic diseases. Due to the extremely large number of included exposure types/settings and neoplasm combinations, we decided to present the review findings in two separate papers. In the first one we addressed the most investigated exposure-outcome pairs (e.g. glioma, meningioma, acoustic neuroma in relation to mobile phone use, or risk childhood leukemia in relation to environmental exposure from fixed-site transmitters) (Karipidis et al., 2024). Here, we report on less researched neoplasms, which include lymphohematopoietic system tumours, thyroid cancer and oral cavity/pharynx cancer, in relation to wireless phone use, or occupational RF exposure. METHODS: Eligibility criteria: We included cohort and case-control studies of neoplasia risks in relation to three types of exposure to RF-EMF: 1. exposure from wireless phone use; 2. environmental exposure from fixed-site transmitters; 3. occupational exposures. In the current paper, we focus on less researched neoplasms including leukaemia, non-Hodgkin's lymphoma and thyroid cancer in mobile phone users; lymphohematopoietic system tumours and oral cavity/pharynx cancer in exposed workers. We focussed on investigations of specific neoplasms in relation to specific exposure sources (termed exposure-outcome pair, abbreviated E-O pairs), noting that a single article may address multiple E-O pairs. INFORMATION SOURCES: Eligible studies were identified by predefined literature searches through Medline, Embase, and EMF-Portal. Risk-of-bias (RoB) assessment: We used a tailored version of the Office of Health Assessment and Translation (OHAT) RoB tool to evaluate each study's internal validity. Then, the studies were classified into three tiers according to their overall potential for bias (low, moderate and high) in selected, predefined and relevant bias domains. DATA SYNTHESIS: We synthesized the study results using random effects restricted maximum likelihood (REML) models. Evidence assessment: Confidence in evidence was assessed according to the Grading of Recommendations, Assessment, Development and Evaluations (GRADE) approach. RESULTS: We included 26 articles, which were published between 1988 and 2019, with participants from 10 countries, reporting on 143 different E-O pairs, including 65 different types of neoplasms. Of these, 19 E-O pairs satisfied the criteria for

inclusion in quantitative syntheses of the evidence regarding the risks of leukaemia, non-Hodgkin's lymphoma or thyroid cancer in relation to mobile phone use, and the risks of lymphohematopoietic system tumours or oral cavity/pharynx cancer following occupational exposure to RF-EMF. RF-EMF exposure from mobile phones (ever or regular use vs no or non-regular use) was not associated with an increased risk of leukaemia [meta-estimate of the relative risk (mRR) = 0.99, 95 % CI 0.91-1.07, 4 studies), non-Hodgkin's lymphoma (mRR = 0.99, 95 % CI = 0.92-1.06, 5 studies), or thyroid cancer (mRR = 1.05, 95 % CI = 0.88-1.26, 3 studies). Long-term (10 + years) mobile phone use was also not associated with risk of leukaemia (mRR = 1.03, 95 % CI 0.85-1.24, 3 studies), non-Hodgkin lymphoma (mRR = 0.99, 95 % CI 0.86-1.15, 3 studies), or thyroid cancer (no pooled estimate given the small number of studies). There were not sufficient studies of any specific neoplasms to perform dose-response meta-analyses for either cumulative call time or cumulative number of calls; individual studies did not show statistically significant associations between lifetime intensity of mobile phone use and any specific neoplasm. Occupational RF-EMF exposure (exposed vs unexposed) was not associated with an increased risk of lymphohematopoietic system tumours (mRR = 1.03, 95 % CI = 0.87-1.28, 4 studies) or oral cavity/pharynx cancer (mRR = 0.68, 95 % CI 0.42-1.11, 3 studies). There were not sufficient studies of any specific neoplasms to perform meta-analysis on the intensity or duration of occupational RF-EMF exposure; individual studies did not show statistically significant associations with either of those exposure metrics and any specific neoplasms. The small number of studies, and of exposed cases in some instances, hampered the assessment of the statistical heterogeneity in findings across studies in the meta-analyses. Based on the summary risk of bias, most studies included in the quantitative evidence syntheses were classified at moderate risk of bias. The most critical issue was exposure information bias, especially for occupational studies where the exposure characterization was rated at high risk of bias for all included studies. Outcome information bias was an issue in mortality-based occupational cohort studies investigating non-rapidly fatal neoplasms. Further, the healthy subscriber effect, and (at a lesser extent) the healthy worker effect, were identified as plausible explanations of the decreased risks observed in some studies. The association of RF-EMF exposure from wireless phone use, or workplace equipment/devices, with other important neoplasms was reported by only one or two studies per tumour, so no quantitative evidence syntheses were conducted on these outcomes. It is noted that there were generally no statistically significant exposure-outcome associations for any combinations, independently of the exposure metric and level, with a few studies reporting decreased risks (especially for smoking-related cancers). There was only one study which assessed the effect of RF-EMF exposure from fixed-site transmitters on less researched neoplasms and it reported no statistically significant associations between exposure from base stations and risk of lymphomas overall, lymphoma subtypes, or chronic lymphatic leukaemia in adults. CONCLUSIONS: For near field RF-EMF exposure to the head from mobile phones, there was low certainty of evidence that it does not increase the risk of leukaemia, non-Hodgkin's lymphoma or thyroid cancer. For occupational RF-EMF exposure, there was very low certainty of evidence that it does not increase the risk of lymphohematopoietic system tumours or oral cavity/pharynx cancer. There was not sufficient evidence to assess the effect of whole-body far-field RF-EMF exposure from fixed-site transmitters (broadcasting antennas or base stations), or the effect of RF-EMF from any source on any other important neoplasms. OTHER: This project was commissioned and partially funded by the World Health Organization (WHO). Co-financing was provided by the New Zealand Ministry of Health; the Istituto Superiore di Sanità in its capacity as a WHO Collaborating Centre for Radiation and Health; and ARPANSA as a WHO Collaborating Centre for Radiation Protection. REGISTRATION: PROSPERO CRD42021236798. Published protocol: [(Lagorio et al., 2021) DOI https://doi.org/10.1016/j.envint.2021.106828].

Lien vers l'article

Waveforms of 4G and 5G Radiofrequency Signals: Are Differences Relevant to Biology or Health?

Foster KR, Maxson D, Zollman PM. *Health Phys*. 2025 Apr 1;128(4):332-6.

This Note briefly reviews, at a level that is intended to be accessible to non-specialists, the similarities and differences between waveforms of 4G Long-Term Evolution (4G LTE) and 5G New Radio (5G NR) transmitted by cellular base stations, as a resource for health physicists and others who are engaged in public communication about cellular telephone technologies. Despite the difference in levels of controversy presently existing between 4G LTE (introduced in 2008) and 5G NR (introduced in 2019), the differences in waveform as represented by the baseband waveform are minimal, although 5G NR offers system designers a much wider choice of parameters. Transmitted radiofrequency signals in both technologies appear noise-like, in a frequency range that is narrowly contained in the assigned channel. It is concluded that the modulation differences between 4G LTE and 5G NR are unlikely to have any biological relevance, but the greater range of accessible frequencies in 5G NR suggests the need for further health research, particularly in the 5G FR2 millimeter-wave band.

Lien vers l'article

Reproduction

Aucun article dans ce bulletin.

Dispositifs médicaux implantables

Aucun article dans ce bulletin.